



Tucana B: A Potentially Isolated and Quenched Ultra-faint Dwarf Galaxy at $D \approx 1.4$ Mpc*

David J. Sand¹ , Burçin Mutlu-Pakdil^{2,3} , Michael G. Jones¹ , Ananthan Karunakaran⁴ , Feige Wang^{1,9} , Jinyi Yang^{1,10} , Anirudh Chiti^{2,3} , Paul Bennet⁵ , Denija Crnojević⁶ , and Kristine Spekkens^{7,8} 

¹ Steward Observatory, University of Arizona, 933 North Cherry Avenue, Tucson, AZ 85721-0065, USA; dsand@arizona.edu

² Kavli Institute for Cosmological Physics, University of Chicago, Chicago, IL 60637, USA

³ Department of Astronomy and Astrophysics, University of Chicago, Chicago IL 60637, USA

⁴ Instituto de Astrofísica de Andalucía (CSIC), Glorieta de la Astronomía, E-18008 Granada, Spain

⁵ Space Telescope Science Institute, 3700 San Martin Drive, Baltimore, MD 21218, USA

⁶ University of Tampa, 401 West Kennedy Boulevard, Tampa, FL 33606, USA

⁷ Department of Physics and Space Science, Royal Military College of Canada, P.O. Box 17000, Station Forces Kingston, ON K7K 7B4, Canada

⁸ Department of Physics, Engineering Physics and Astronomy, Queen's University, Kingston, ON K7L 3N6, Canada

Received 2022 May 17; revised 2022 July 15; accepted 2022 July 18; published 2022 August 12

Abstract

We report the discovery of Tucana B, an isolated ultra-faint dwarf galaxy at a distance of $D = 1.4$ Mpc. Tucana B was found during a search for ultra-faint satellite companions to the known dwarfs in the outskirts of the Local Group, although its sky position and distance indicate the nearest galaxy to be ~ 500 kpc distant. Deep ground-based imaging resolves Tucana B into stars, and it displays a sparse red giant branch consistent with an old, metal-poor stellar population analogous to that seen in the ultra-faint dwarf galaxies of the Milky Way, albeit at fainter apparent magnitudes. Tucana B has a half-light radius of 80 ± 40 pc and an absolute magnitude of $M_V = -6.9_{-0.6}^{+0.5}$ mag ($L_V = (5_{-2}^{+4}) \times 10^4 L_\odot$), which is again comparable to the Milky Way's ultra-faint satellites. There is no evidence for a population of young stars, either in the optical color–magnitude diagram or in GALEX archival ultraviolet imaging, with the GALEX data indicating $\log(\text{SFR}_{\text{NUV}}/M_\odot \text{ yr}^{-1}) < -5.4$ for star formation on $\lesssim 100$ Myr timescales. Given its isolation and physical properties, Tucana B may be a definitive example of an ultra-faint dwarf that has been quenched by reionization, providing strong confirmation of a key driver of galaxy formation and evolution at the lowest mass scales. It also signals a new era of ultra-faint dwarf galaxy discovery at the extreme edges of the Local Group.

Unified Astronomy Thesaurus concepts: Dwarf galaxies (416); Quenched galaxies (2016); Galaxy quenching (2040)

Supporting material: data behind figure

1. Introduction

The faint end of the galaxy luminosity function is important for understanding dark matter and astrophysics on small scales (see, e.g., Bullock & Boylan-Kolchin 2017; Simon 2019, for recent reviews). In the Local Group, observations continue to find a variety of ultra-faint galaxies (for instance, most recently Mau et al. 2020; Cerny et al. 2021, 2022), while numerical simulations work out how stars form in the smallest dark matter subhalos of Milky Way–like systems (e.g., Brooks et al. 2013; Sawala et al. 2016; Wetzel et al. 2016; Samuel et al. 2020; Applebaum et al. 2021; Engler et al. 2021). Outside of the Local Group, faint dwarf galaxies are being identified in resolved stars (Chiboucas et al. 2013; Crnojević et al. 2014; Sand et al. 2014; Crnojević et al. 2016b; Carlin et al. 2016; Toloba et al. 2016; Smercina et al. 2018; Bennet et al. 2019; Crnojević et al. 2019; Bennet et al. 2020; Mutlu-Pakdil et al.

2022), diffuse or semiresolved light (e.g., Bennet et al. 2017; Carlsten et al. 2020; Davis et al. 2021), as well as spectroscopic surveys (Geha et al. 2017; Mao et al. 2021). These programs are leading to a new understanding of both the scatter in satellite properties as well as potential challenges to our picture of galaxy formation on small scales (Bennet et al. 2019, 2020; Carlsten et al. 2021; Karunakaran et al. 2021; Smercina et al. 2022).

Despite this progress, there are still regions of dwarf galaxy discovery space that are largely unexplored. In particular, only a handful of new dwarfs have been uncovered at the periphery of the Local Group and its immediate environs ($D \approx 0.5$ – 2.0 Mpc). Examples include the star-forming and relatively isolated dwarf Leo P ($D = 1.6$ Mpc, $M_V = -9.3$ mag; Giovanelli et al. 2013; Rhode et al. 2013; McQuinn et al. 2015) and the gas-bearing dwarf Antlia B ($D = 1.35$ Mpc, $M_V = -9.7$ mag; Sand et al. 2015a; Hargis et al. 2020), both of which are members of the NGC 3109 dwarf association. There is also KKR 25, an isolated dwarf spheroidal with no signs of recent star formation or neutral gas ($D = 1.9$ Mpc, $M_V = -10.9$ mag; Makarov et al. 2012). A significant population of faint dwarf galaxies is expected at the edge of the Local Group (e.g., Tollerud & Peek 2018), although recent searches (mostly looking for stellar counterparts to compact, high-velocity HI clouds) have come up short and only discovered examples of more distant, isolated dwarfs (Adams et al. 2013; Sand et al. 2015b;

* This paper includes data gathered with the 6.5 m Magellan Telescope at Las Campanas Observatory, Chile.

⁹ NASA Hubble Fellow.

¹⁰ Strittmatter Fellow.



Bellazzini et al. 2015; Tollerud et al. 2015, 2016; Bennet et al. 2022).

Of particular interest are further examples of quenched dwarf galaxies at the edge of the Local Group. This includes relatively bright objects like Tucana ($M_V = -9.5$; $D = 890$ kpc) and Cetus ($M_V = -11.2$; $D = 700$ kpc), which are potential “backsplash” systems that were plausibly quenched and stripped of their gas after interacting with the Milky Way and have subsequently passed back out of the Local Group (e.g., Teyssier et al. 2012; Buck et al. 2019)—these objects tell us about the orbital evolution of the Milky Way satellite system. Beyond the true edge of the Local Group ($\sim 2\text{--}2.5 r_{200}$, or $\sim 750\text{--}1000$ kpc), it becomes less and less likely that a dwarf galaxy has had a past interaction with the Milky Way (Buck et al. 2019), and it is in this regime where true “field” dwarfs can be found. Quenched, field dwarfs in the ultra-faint dwarf galaxy regime may cease forming stars not because of any interaction with a larger galaxy but due to reionization (Babul & Rees 1992; Bullock et al. 2000; Benson et al. 2002; Ricotti & Gnedin 2005; Jeon et al. 2017; Applebaum et al. 2021) or other internal mechanisms, such as supernova feedback (e.g., Dekel & Silk 1986; Mac Low & Ferrara 1999). The discovery of such systems would provide a strong verification of galaxy formation models on small scales.

Here we report the discovery of Tucana B, which to our knowledge is the first quenched, isolated ultra-faint dwarf galaxy identified in the extreme outskirts of the Local Group. The name Tucana B was chosen because of its constellation and the prior existence of the Tucana dwarf spheroidal; a similar naming convention has been used for other dwarfs at the edge of the Local Group (e.g., Sextans A and B; Antlia and Antlia B). We present this new discovery in Section 2, and discuss follow-up optical observations in Section 3. In Section 4 we measure the basic physical properties of Tucana B and present an analysis of its stellar population. In Section 5 we place Tucana B into context with the satellites of the Milky Way and other dwarfs in the outskirts of the Local Group. In particular, we discuss the environment and isolation of Tucana B and the ramifications for reionization as a viable quenching mechanism. We summarize and look ahead in Section 6.

2. Discovery of Tucana B

Tucana B was found during a visual search for faint dwarf galaxy companions to the distant dwarf spheroidal galaxy Tucana (Lavery & Mighell 1992), at $D = 890$ kpc (Bernard et al. 2009) and $M_V = -9.5$ (Saviane et al. 1996). To do this, we used data from the DESI Legacy Imaging Surveys Data Release 9 (Dey et al. 2019) and their interactive color image viewer.¹¹ We uploaded a custom file to mark off a region with projected radius of 100 kpc (≈ 6.4 at the distance of Tucana) and searched for visual overdensities of resolved stars with underlying diffuse light, indicative of a dwarf galaxy at the edge of the Local Group. The field was inspected at a variety of spatial scales and contrast levels.

Tucana B stood out during the search and is partially resolved into stars in the Legacy Imaging Survey viewer (Figure 1). Tucana B is in the footprint of the Dark Energy Survey Data Release 2 (DES DR2; Abbott et al. 2021), and we downloaded photometry of the field using NOIRLab’s Query

Interface Tool.¹² Tucana B is not well resolved in the DES g -band data, but has r - and i -band photometry suggestive of a resolved stellar population with an old, metal-poor red giant branch (RGB). Given this, we sought deeper ground-based optical data, which we present below.

Tucana B is located $\sim 6^\circ$ from the Tucana dwarf spheroidal and is ~ 500 kpc more distant along the line of sight (we derive a distance of $D = 1.4$ Mpc to Tucana B in Section 4.1), and so we provisionally conclude that the two systems are not physically associated. Further, we have performed a careful, final visual search of a 200×200 kpc² region centered on Tucana B at our inferred distance and have not identified additional resolved dwarf candidates. We discuss the environment of Tucana B in Section 5.

3. Deep Optical Follow-up

Deep g - and r -band imaging was taken with the Inamori-Magellan Areal Camera & Spectrograph (IMACS; Dressler et al. 2006) on 2021 December 03 (UT). We used the $f/2$ camera, which delivers a ~ 27.4 field of view and $0''.2$ pixel⁻¹ scale. Observations were taken in the g (4×300 s) and r (3×300 s) bands, with small dithers between exposures. The data were reduced in a standard way (similar to that in Chiti et al. 2020), which included overscan subtraction and flat-fielding, followed by an astrometric correction using a combination of ASTROMETRY.NET (Lang et al. 2010) and SCAMP (Bertin 2006). Final image stacking was accomplished with SWARP (Bertin 2010) using a weighted average of the input images. The final g - and r -band stacked images have point-spread function FWHM values of $0''.8$ and $0''.9$, respectively. We display the final, stacked r -band IMACS imaging in the right panel of Figure 1.

We performed point-spread function fitting photometry on the stacked IMACS images, using DAOPHOT and ALLFRAME (Stetson 1987, 1994), following the general procedure described in Mutlu-Pakdil et al. (2018). The photometry was calibrated to point sources in the DES DR2 catalog (Abbott et al. 2021), including a color term, and was corrected for Galactic extinction (Schlafly & Finkbeiner 2011) on a star by star basis. The typical color excess at the position of Tucana B is $E(B - V) = 0.018$ mag. In the remainder of this work we present dereddened g_0 and r_0 magnitudes.

To determine our photometric errors and completeness as a function of magnitude and color, we conduct artificial star tests with the DAOPHOT routine ADDSTAR, similar to previous work (Sand et al. 2012; Mutlu-Pakdil et al. 2018). Over several iterations, we injected $\sim 10^5$ artificial stars into our stacked images (a factor of ~ 2 more than the number of point sources in the original image) with a range of magnitudes ($r = 18\text{--}29$ mag) and colors ($g - r = -0.5\text{--}1.5$) and then photometered the simulated data in the same way as the original images. The 50% (90%) completeness level was at $r = 25.9$ (24.5) and $g = 26.4$ (25.1) mag. In Figure 2 we show the color-magnitude diagram (CMD) of Tucana B within 1.33 half-light radii r_h (as derived in Section 4.3), along with several equal-area background CMDs. We discuss the structure and stellar populations of Tucana B in the following section.

¹¹ <https://www.legacysurvey.org/viewer>

¹² <https://datalab.noirlab.edu/query.php>

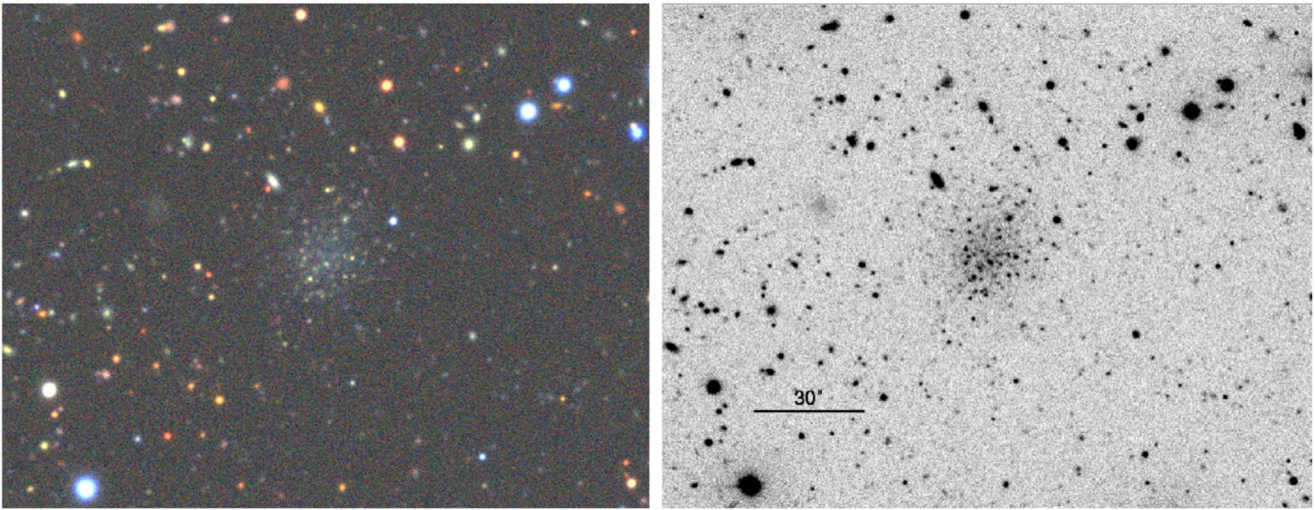


Figure 1. Tucana B as seen in the DESI Legacy Imaging Surveys sky browser (left) and in the deeper Magellan r -band IMACS data (right), where it is more clearly resolved into stars. North is up and east is to the left. The diffuse object to the east of Tucana B is likely a background dwarf galaxy associated with a galaxy group at $z = 0.036$ (Díaz-Giménez & Zandivarez 2015), which is centered to the northeast and has several other similar, diffuse objects associated with it.

4. Properties of Tucana B

In this section, we measure the physical properties of Tucana B using our new Magellan photometry, as well as archival HI and GALEX UV data sets.

4.1. Distance

As we discuss below, the CMD of Tucana B seems to display a stellar population consisting of a sparsely populated old, metal-poor RGB (Figure 2). A challenge for measuring the distance to Tucana B is the lack of a well-defined tip of the RGB because of its intrinsic faintness, where few or no stars populate the upper regions of the RGB, as has been discussed in several previous works (e.g., Madore & Freedman 1995; Weisz et al. 2019; Carlin et al. 2021; Mutlu-Pakdil et al. 2022). The ground-based data are also too shallow to identify a horizontal branch or any associated RR Lyrae stars, both of which could provide distance estimates.

Instead of using a tip of the RGB-derived distance, we measure the distance to Tucana B using a CMD-fitting technique, comparing the number of stars consistent with several old, metal-poor theoretical isochrones and adopting a methodology similar to that used for several of the Milky Way ultra-faint dwarfs (e.g., Walsh et al. 2008; Sand et al. 2009). We use the Dartmouth isochrones (Dotter et al. 2008), focusing on tracks with stellar ages of 13.5 Gyr and low metallicities ($[\text{Fe}/\text{H}]$ of -2.5 , -2.0 , and -1.5). We include all Tucana B stars with $r_0 < 25.5$ mag within $0'.35$ of its center, which visually encapsulates the bulk of its main body. Each isochrone fiducial is shifted through 0.025 mag intervals in distance modulus ($m - M$) from 24.5 to 27.0 mag (~ 0.8 – 2.5 Mpc). At each of these steps, the number of stars consistent with the fiducial is tabulated. The selection region for stars to be counted is simply defined by two red/blue boundaries in $(g - r)_0$ color for a given r_0 magnitude, as determined by the uncertainties found in our artificial star tests. Background stars are also accounted for by running the identical procedure over an appropriately scaled background region and then subtracting this number from that of the Tucana B selection. Implicit in this technique is the assumption that Tucana B has a single-age,

exclusively old (~ 13.5 Gyr) stellar population. We have not explored other isochrone model tracks from different groups, or at different ages, which may expand the allowed distance range discussed below. We also assume no internal extinction associated with Tucana B and only include a Milky Way component.

The best-fit distance moduli for the 13.5 Gyr, $[\text{Fe}/\text{H}] = -2.0$ and -2.5 isochrones are $m - M = 25.6$ and 25.9 mag ($D = 1.3$ and 1.5 Mpc), respectively. We found the best-fit distance for the 13.5 Gyr, $[\text{Fe}/\text{H}] = -1.5$ isochrone unsatisfactory, implying a distance too nearby and too red to properly match the data (see discussion in the next paragraph). Given the two satisfactory matches for a very metal-poor population, we take the mean of those two measurements as our distance modulus ($m - M = 25.75$; $D = 1.4$ Mpc) and continue to discuss our uncertainties below.

Given the projected proximity of Tucana B to the original Tucana dwarf spheroidal galaxy, which is at $D = 900$ kpc, we overplot an old metal-poor isochrone (13.5 Gyr, $[\text{Fe}/\text{H}] = -2.5$) at that distance onto the CMD in Figure 2. From this, it is clear that Tucana B is at a larger distance than the original Tucana dwarf; otherwise, it would imply that the upper 1–2 mag of the RGB in Tucana B was completely unpopulated. Thus, the two objects are not likely physically associated, and the lower distance limit to Tucana B is greater than 900 kpc.

As another point of discussion, inspection of the CMD shows three stars at $r_0 \approx 22.7$ – 23.0 and $(g - r)_0 \approx 1.1$; the membership status and provenance of these stars is important for assessing the distance of Tucana B. First, aside from our baseline assumption that these stars are upper RGB members, these stars may be asymptotic giant branch (AGB) stars associated with Tucana B itself, which would imply that the brightest RGB stars are at $r_0 \approx 23.5$ mag. Alternatively, these stars could be foreground stars, although there are very few contaminant stars at that position in color–magnitude space (see right panels of Figure 2). In either, it may imply a larger distance to Tucana B, although we discount this possibility because it does not match the data. We overplot the same 13.5 Gyr, $[\text{Fe}/\text{H}] = -2.5$ isochrone, but at a distance of $D = 2.0$ Mpc, corresponding to a scenario where the three stars at $r_0 \approx 22.7$ – 23.0 are either foreground contaminants or

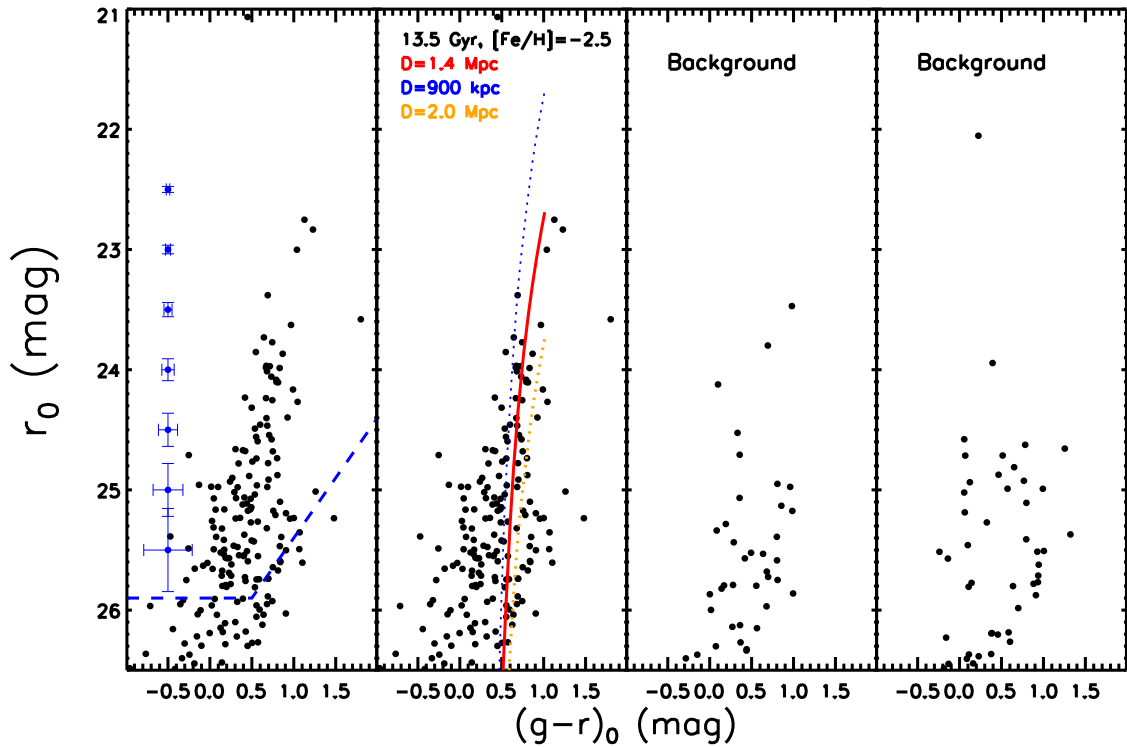


Figure 2. The CMD of Tucana B from our Magellan IMACS data (see Section 3). In the two left panels, we display the CMD of Tucana B within $1.33 r_h$ ($16''$). Along the left side of the far-left CMD are the typical uncertainties at different r -band magnitudes, as determined by artificial star tests. The dashed line marks the 50% completeness limit. In the center-left panel, we plot 13.5 Gyr, $[\text{Fe}/\text{H}] = -2.5$ isochrones (Dotter et al. 2008) at different distances. The blue dotted isochrone is at the distance of the original Tucana dwarf spheroidal ($D = 900$ kpc), while the orange isochrone is at a distance of 2 Mpc. The two panels on the right show randomly selected equal-area background regions. There is likely significant background galaxy contamination at $r_0 \gtrsim 24.5$ mag.

(The data used to create this figure are available.)

AGB stars. While this isochrone roughly matches the putative magnitude of the tip of the RGB in this scenario, it is skewed redward of the main locus of Tucana B stars and cannot be pushed further blueward as it would imply an unrealistically low metallicity for Tucana B. For this reason, Tucana B must be at a closer distance than 2 Mpc, and the three bright aforementioned stars are not likely to be AGB stars or exclusively foreground contaminants.

To determine a distance uncertainty to Tucana B more concrete than the broad limits discussed above, we carefully moved old, metal-poor isochrones (both 13.5 Gyr, $[\text{Fe}/\text{H}] = -2$ and -2.5) by eye through different distances around our best fit of $m - M = 25.75$ ($D = 1.4$ Mpc) and noted where clear departures between isochrone and data occur. For distances much closer than $m - M = 25.75$, the isochrones would imply a completely unpopulated upper RGB, and the three stars at $r_0 \approx 22.7\text{--}23.0$ become too red to match a metal-poor isochrone. From this inspection, we estimate a lower distance limit of $m - M = 25.3$ ($D = 1.1$ Mpc). For distances farther than $m - M = 25.75$, we were most concerned about the isochrone skewing redwards of the data, without much concern for the three stars at $r_0 \approx 22.7\text{--}23.0$ as these may be contaminants or member AGB stars in this scenario, as discussed above. This leads to a visual upper distance limit of $m - M = 26.3$ ($D = 1.8$ Mpc). While we emphasize that space-based data down to the horizontal branch is necessary for a definitive distance to Tucana B, the ground-based CMD indicates a $m - M = 25.75^{+0.55}_{-0.45}$ mag ($D = 1.4^{+0.4}_{-0.3}$ Mpc).

4.2. Stellar Population

Based on the CMD and our distance constraints, Tucana B appears to only consist of an old metal-poor stellar population (Figure 2). Other recently discovered dwarfs at the edge of the Local Group, such as Leo P ($M_V = -9.3$) and Antlia B ($M_V = -9.7$), have clear signs of star formation in the form of blue main-sequence stars (McQuinn et al. 2015; Hargis et al. 2020), but any plausible blue member stars in Tucana B are small in number and consistent with background contamination (Figure 2). Its CMD is most analogous to the ultra-faint dwarf galaxies of the Milky Way, which only consist of an old stellar population, with the exception of Leo T (de Jong et al. 2008; Weisz et al. 2012).

To further assess any possible young stellar population, we search for coincident UV emission with data from the Galaxy Evolution Explorer (GALEX; Martin et al. 2005) archive, which is sensitive to star formation on $\lesssim 100$ Myr timescales (e.g., Lee et al. 2011). We adopt the methodology of Karunakaran et al. (2021), using a $16''$ aperture ($1.33 r_h$), finding no detection at the position of Tucana B. We assess our detection limits by placing 1000 random apertures over the GALEX field (after masking bright objects). We then translate these NUV and FUV flux limits to star formation rate limits using the relations of Iglesias-Páramo et al. (2006), finding $\log(\text{SFR}_{\text{NUV}}/M_\odot \text{ yr}^{-1}) < -5.4$ and $\log(\text{SFR}_{\text{FUV}}/M_\odot \text{ yr}^{-1}) < -6.0$, respectively. Both limits are more than an order of magnitude more stringent than nearly all UV detections in satellite galaxies around Milky Way-like halos

Table 1
Tucana B Properties

Parameter	Value
α_0 (J2000)	22:47:00.5 \pm 1''5
δ_0 (J2000)	-58:24:27.0 \pm 2''3
$m - M$ (mag)	25.75 $^{+0.55}_{-0.45}$
Distance (Mpc)	1.4 $^{+0.4}_{-0.3}$
M_V (mag)	-6.9 $^{+0.5}_{-0.6}$
L_V (L_\odot)	(5 $^{+4}_{-2}$) $\times 10^4$
r_h (arcsec)	12 \pm 5
r_h (pc)	80 \pm 40
ϵ	<0.35
$\log(\text{SFR}_{\text{NUV}}/M_\odot \text{ yr}^{-1})$	<-5.4
$\log(\text{SFR}_{\text{FUV}}/M_\odot \text{ yr}^{-1})$	<-6.0
$\log(M_{\text{HI}}/M_\odot)$	<5.6

(e.g., Karunakaran et al. 2021), again emphasizing the lack of star formation in Tucana B.

It is important to note that the current data set cannot rule out the presence of a faint intermediate age stellar population, greater than ~ 500 Myr old. Such intermediate-age stellar populations do exist in faint dwarf galaxies in the Local Group, for instance, in the Hubble Space Telescope (HST) imaging of Andromeda XVI (Weisz et al. 2014b). To be sensitive to such stellar populations will require deep space-based observations, as we continue to emphasize in this work.

4.3. Stellar Structure and Luminosity

Tucana B is a distant stellar system with only ~ 100 resolved stars in our Magellan/IMACS data. As in previous work on similarly sparse systems (e.g., Sand et al. 2014), we fit an exponential profile to the two-dimensional distribution of stars consistent with the RGB of Tucana B using the maximum likelihood technique of Martin et al. (2008). We select stars for this analysis that are consistent with the best-fitting Dartmouth isochrone, at a distance of $D = 1.4$ Mpc as found in Section 4.1, after taking into account the photometric uncertainties for stars brighter than the 50% completeness limit. The fit includes the central position (α_0, δ_0), position angle (θ), ellipticity (ϵ), half-light radius (r_h), and a constant background surface density as free parameters. Uncertainties on each parameter were calculated through a bootstrap resampling analysis, with 1000 iterations. As a check on our results, we repeated the calculations while only including RGB stars down to $r_0 = 25.4$ mag, a half-magnitude brighter than our initial iteration; the derived structural parameters did not change to within the uncertainties.

The results of the structural analysis are shown in Table 1. Tucana B has a half-light radius of 80 ± 40 pc (this includes our distance uncertainty). Its ellipticity is not well constrained: We find an upper limit of <0.35 at 95% confidence, reinforcing the roughly circular shape of the dwarf seen in Figure 1. Given this, no constraint on the position angle is possible. The central position of the new dwarf is constrained to a couple of arcseconds.

To derive the luminosity of Tucana B, we employ the methodology of Martin et al. (2008), which is appropriate for faint dwarf galaxies in the ‘‘CMD shot noise’’ regime, where the presence or absence of individual stars in the upper RGB can greatly influence the overall luminosity. First, we build a well-populated CMD by using a $[\text{Fe}/\text{H}] = -2$, 13.5 Gyr isochrone and a Salpeter initial mass function. We convolve this with our

measured completeness and photometric uncertainties, shifted to $D = 1.4$ Mpc. We then randomly selected the same number of stars from the simulated CMD as was found in our maximum likelihood analysis, taking into account the luminosity in the simulated population below our detection limit. We repeat this process 100 times, taking the median and standard deviation as our final absolute magnitude and uncertainty (we also add the distance uncertainty in quadrature for our final absolute magnitude uncertainty). We convert to the V band using the filter transformation equations of Jordi et al. (2006) and ultimately find $M_V = -6.9^{+0.5}_{-0.6}$ mag ($L_V = (5^{+4}_{-2}) \times 10^4 L_\odot$). Based on this, Tucana B is a true ultra-faint dwarf galaxy, similar in luminosity to Eridanus II (Crnojević et al. 2016a).

4.4. Gas Content

Given the isolation and apparent lack of recent star formation in Tucana B, it is important to assess its neutral gas content. The deepest available HI observations in the direction of Tucana B are from the Galactic All Sky Survey (GASS; McClure-Griffiths et al. 2009; Kalberla et al. 2010; Kalberla & Haud 2015), with the caveat that these observations only extend to a redshift of $\sim 500 \text{ km s}^{-1}$. Tucana B is located in a field surrounded by complex foreground HI features associated with the Milky Way and Magellanic Clouds (e.g., Westmeier 2018). This complicates the search for a HI counterpart of Tucana B as, without an a priori redshift, any HI emission along the line of sight could be associated with the Milky Way. Although difficult, it will be important to measure a stellar velocity for Tucana B for this task.

In the GASS data, there is a clump of HI emission that peaks approximately $20'$ to the SW of Tucana B (note that the spatial resolution of the GASS data is $16'$). This clump (at $cz_\odot \approx 220 \text{ km s}^{-1}$) forms a distinct, almost point-like (at the resolution of GASS) feature, but is surrounded by Milky Way emission. Therefore, it is highly likely that this feature is merely associated with the Milky Way and not Tucana B, but we cannot robustly exclude either option with the available data.

There is no other candidate feature in the GASS data; therefore, if we assume this feature is not associated with Tucana B, then we can proceed to set an upper limit on its HI mass. The typical rms noise of GASS is 53 mK in 0.82 km s^{-1} channels. Approximating the Parkes radio telescope gain as 0.7 K/Jy gives a 3σ sensitivity of $\log(M_{\text{HI}}/M_\odot) < 5.6$ for a source of 20 km s^{-1} velocity width and a distance of 1.4 Mpc. Future high-resolution, interferometric observations, potentially with MeerKAT or the Australia Telescope Compact Array (ATCA), are necessary to further constrain the HI content of Tucana B.

5. Discussion

Tucana B is a unique discovery for a dwarf galaxy just beyond the Local Group, given both its luminosity, isolation, and its lack of apparent star formation or neutral gas. Here we discuss the physical properties and environment of Tucana B in the broader context of faint dwarf galaxies as a population.

5.1. Local Group and Isolated Dwarf Comparisons

In Figure 3 we plot a size–luminosity relation featuring the satellites of the Milky Way, along with quenched dwarfs in the outskirts of the Local Group. We also highlight Eridanus II,

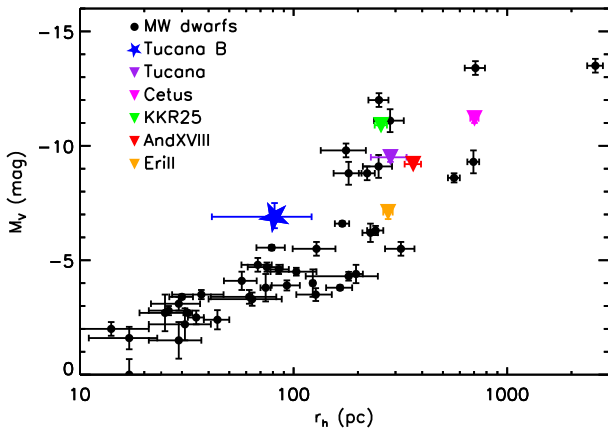


Figure 3. Absolute magnitude as a function of half-light radius of Tucana B and other isolated, quenched dwarfs in the outskirts of the Local Group (Cetus: McConnachie & Irwin 2006; Tucana: Saviane et al. 1996; And XVIII: McConnachie et al. 2008; KKR25: Makarov et al. 2012; Eri II: Crnojević et al. 2016a). Also plotted are the dwarf satellites of the Milky Way (McConnachie 2012; Carlin et al. 2017; Muñoz et al. 2018; Mutlu-Pakdil et al. 2018). Tucana B is the faintest and smallest of the isolated, quenched Local Group dwarfs.

which is situated near the virial radius of the Milky Way itself but is devoid of recent star formation and gas.

In comparison to the Milky Way satellites, Tucana B has a luminosity similar to Eridanus II (Crnojević et al. 2016a; Simon et al. 2021) and is slightly more luminous than the ultra-faint dwarfs Boötes I ($M_V = -6.0$ mag; Muñoz et al. 2018) and Hercules ($M_V = -6.2$ mag; Sand et al. 2009). Interestingly, Tucana B is significantly more compact than either of these systems, which have half-light radii $\gtrsim 200$ pc. Its half-light radius is comparable to much fainter satellites such as Canes Venatici II ($M_V \approx -4.6$ mag; $r_h \approx 85$ pc; Sand et al. 2012).

Despite its compact nature for its luminosity, Tucana B is only a mild outlier in comparison to the Milky Way dwarf population as a whole, especially considering its large uncertainties. If a larger population of field ultra-faint dwarfs display a more compact stellar distribution than their counterparts near the Milky Way, it may point to dwarf mergers, tidal encounters, or similar mechanisms puffing up the stellar distribution in the Milky Way sample (e.g., Frings et al. 2017; Chiti et al. 2021; Tarumi et al. 2021), although this is just speculation at this point.

5.2. Environment

To investigate the environment of Tucana B, we plot the known dwarfs and galaxies of the Local Volume in two projections of the supergalactic coordinate system in Figure 4. We focus on the supergalactic X - Y projection, as the Y - Z plot simply shows the local plane of galaxies used to roughly define the supergalactic coordinate system; note that Tucana B is on this plane. Given our search area, it is no surprise that the nearest galaxy to Tucana B is the original Tucana dwarf, at a physical separation of ~ 500 kpc, followed by the low-mass galaxy IC 5152 (~ 620 kpc separation). Both of these separations are beyond the virial radius of either low-mass galaxy (even with the considerable Tucana B distance uncertainties). As mentioned elsewhere, it will be important to measure a velocity to Tucana B to further assess whether it interacted with either low-mass system in the past. Tucana B is also well beyond the virial radius of the Milky Way itself,

which is between $r_{\text{vir}} = 200$ – 300 kpc (e.g., Klypin et al. 2002; Putman et al. 2021), putting it at $\gtrsim 4.5 r_{\text{vir}}$. Barring future discoveries, Tucana B is one of the most isolated galaxies within ~ 2 Mpc.

5.3. The Nature of Tucana B

Tucana B is an apparently quenched, isolated ultra-faint dwarf galaxy, which may have deep implications for our view of low mass galaxy formation, depending on its origins.

First, it is possible that Tucana B is a so-called backplash galaxy and may have had a previous encounter with the Milky Way, quenching its star formation and stripping it of its gas before being ejected out to large galactocentric radii. Several systems in the outskirts of the Local Group have been identified as possible backplash systems (see, for instance, Table 4 in Buck et al. 2019, for one sample). In order to fully assess this scenario, a velocity measurement of Tucana B is necessary, and both a stellar velocity measurement and deeper H I observations should be prioritized. Nonetheless, simulations suggest it is very unlikely that Tucana B is a backplash system, as most such galaxies should be at $\lesssim 2.5 r_{\text{vir}}$ (e.g., Teyssier et al. 2012; Diemer & Kravtsov 2015; Buck et al. 2019; Applebaum et al. 2021), which is significantly closer to the Milky Way than Tucana B.

It is also possible that Tucana B is a faint example of a transition dwarf galaxy, which exhibit H I emission but show no signs of recent star formation (Skillman et al. 2003; Weisz et al. 2011), possibly because they are in between star formation episodes (see e.g., El-Badry et al. 2016). While no H I emission is detected in Tucana B, more stringent limits are necessary to rule out this scenario (preferably down to $M_{\text{HI}}/L_V \approx 1$; e.g., Putman et al. 2021), along with deeper photometry to probe intermediate age star formation events.

As the backplash scenario is unlikely, it points to Tucana B being a true quenched field ultra-faint dwarf galaxy (again with the caveat that deeper optical and H I data are necessary). Without any interaction with the hot halo or gravitational field of a massive galaxy, reionization and/or some other internal mechanism (i.e., supernova feedback) is likely responsible for the gas-free and quenched status of Tucana B. Such a scenario is seen in recent simulations of field dwarf galaxies (e.g., Jeon et al. 2017; Rey et al. 2020; Applebaum et al. 2021), although even here it is possible for faint dwarf galaxies to be quenched by other mechanisms, such as ram pressure stripping by gas in the cosmic web itself (e.g., Benítez-Llambay et al. 2013).

It has long been recognized that reionization can essentially “boil” the gas out of the dark matter potential wells of ultra-faint dwarf galaxies, explaining their dearth of stars and the possibility that some dark matter halos never form stars at all (e.g., Babul & Rees 1992; Bullock et al. 2000; Benson et al. 2002; Ricotti & Gnedin 2005). Observations of the ultra-faint dwarfs around the Milky Way lend support to this picture, as HST observations down to the oldest main-sequence turnoff reveal nearly synchronous star formation at very early times (~ 13 Gyr ago), with little to no star formation since the reionization epoch (Weisz et al. 2014a; Brown et al. 2014). However, as the Milky Way ultra-faint dwarfs have also experienced its hot halo and significant tidal forces, it is difficult to distinguish between all of these mechanisms as the primary source for their quenched, gas-free status. Thus, Tucana B may provide strong confirmation of reionization’s

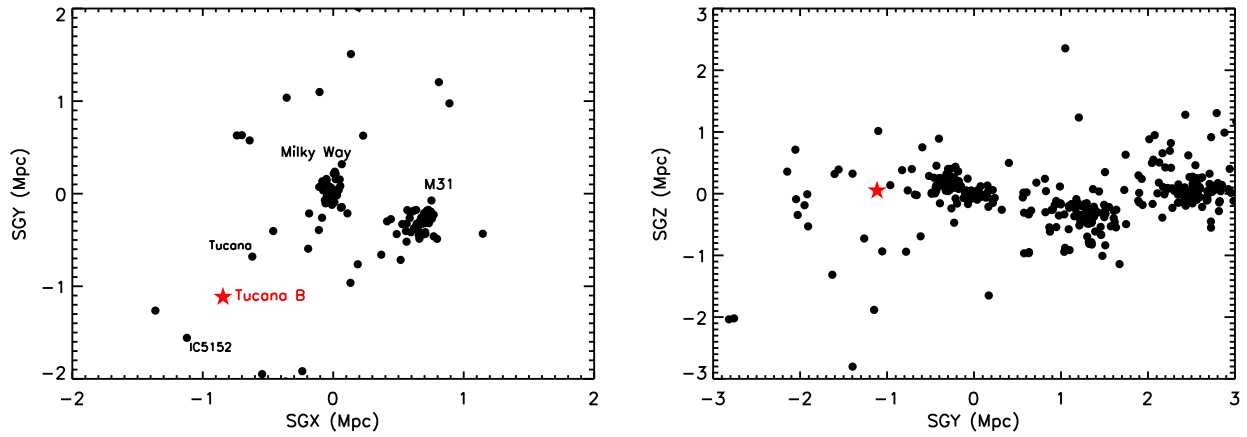


Figure 4. A map of nearby galaxies (from the updated, online version of the Catalog of Neighboring Galaxies; Karachentsev et al. 2004) in supergalactic coordinates, highlighting the isolation of Tucana B. Left: In the supergalactic X - Y plane, looking down on the local plane of galaxies, Tucana B is clearly isolated, with its nearest neighbor being the original Tucana dwarf, at a physical separation of ~ 500 kpc. The Large Magellanic Cloud-sized galaxy IC 5152 is separated by ~ 620 kpc (at $D \approx 2$ Mpc; Karachentsev et al. 2002). These quoted separations are in 3D space, not just in the supergalactic X - Y plane. Right: We show the supergalactic Y - Z plane, which is defined by the local plane of galaxies, used to roughly define the supergalactic coordinate system.

role in influencing galaxy formation and evolution at the lowest mass scales.

6. Summary and Future Outlook

We have presented the discovery of Tucana B, an ultra-faint dwarf galaxy in the extreme outskirts of the Local Group ($D \approx 1.4$ Mpc). Its luminosity ($M_V = -6.9$ mag) and apparent lack of star formation and neutral gas make it unique among recent discoveries at this approximate distance (e.g., Makarov et al. 2012; Giovanelli et al. 2013; Sand et al. 2015a). The isolation of Tucana B also suggests that its star formation was quenched by reionization or some other internal mechanism, rather than interaction with a larger galaxy halo, although further data is necessary to solidify these results. Even if it is found that Tucana B has an intermediate-age stellar population or contained a reservoir of H I gas, it will still be a novel ultra-faint dwarf with properties distinct from those found around the Milky Way. It is likely that similar systems to Tucana B are waiting to be discovered, although its semiresolved status in the discovery DECam data point to the need for a tailored search. A complete census of such objects is necessary to understand the demographics of the field ultra-faint dwarf galaxy population.

Tucana B is a prime target for future space-based follow-up to pin down its structure and star formation history, possibly down to the oldest main-sequence turnoff. In particular, Tucana B may provide a definitive opportunity to understand the role that reionization plays in the quenching of the faintest galaxies. As discussed, HST observations of the Milky Way’s ultra-faint dwarfs down to the oldest main-sequence turnoff reveal early, nearly synchronous star formation (Weisz et al. 2014a; Brown et al. 2014). There are hints that those ultra-faint dwarfs associated with the Magellanic Clouds had a slightly different star formation epoch than those of the Milky Way (Sacchi et al. 2021) and probing further systems and environments is essential for confirming and extending these results. Prior to the advent of the James Webb Space Telescope, similar observations beyond the Local Group were prohibitive, but the Near Infrared Camera (NIRCam) enables such studies out to ~ 2 Mpc (e.g., Weisz & Boylan-Kolchin 2019). Tucana B, and similar systems to be discovered in the near-future (e.g., see predictions and simulated data in Rodriguez Wimberly et al. 2019; Mutlu-Pakdil et al. 2021, respectively),

will be a crucial data set for understanding reionization’s effect on star formation and subsequent cessation in the smallest dark matter halos.

D.J.S. acknowledges support from NSF grants AST-1821967 and 1813708. B.M.P. is supported by an NSF Astronomy and Astrophysics Postdoctoral Fellowship under award AST-2001663. Research by D.C. is supported by NSF grant AST-1814208. A.K. acknowledges financial support from the State Agency for Research of the Spanish Ministry of Science, Innovation and Universities through the “Center of Excellence Severo Ochoa” awarded to the Instituto de Astrofísica de Andalucía (SEV-2017-0709) and through the grant POSTDOC_21_00845 financed from the budgetary program 54a Scientific Research and Innovation of the Economic Transformation, Industry, Knowledge and Universities Council of the Regional Government of Andalusia. F.W. thanks the support provided by NASA through the NASA Hubble Fellowship grant #HF2-51448 awarded by the Space Telescope Science Institute, which is operated by the Association of Universities for Research in Astronomy, Incorporated, under NASA contract NAS5-26555. A.C. is supported by a Brinson Prize Fellowship at UChicago/KICP. K.S. acknowledges support from the Natural Sciences and Engineering Research Council of Canada (NSERC).

This research uses services or data provided by the Astro Data Lab at NSF’s National Optical-Infrared Astronomy Research Laboratory. NOIRLab is operated by the Association of Universities for Research in Astronomy (AURA), Inc. under a cooperative agreement with the National Science Foundation.

The work used images from the Dark Energy Camera Legacy Survey (DECaLS; Proposal ID 2014B-0404; PIs: David Schlegel and Arjun Dey). Full acknowledgment at <https://www.legacysurvey.org/acknowledgment/>.

This research is based on observations made with the Galaxy Evolution Explorer, obtained from the MAST data archive at the Space Telescope Science Institute, which is operated by the Association of Universities for Research in Astronomy, Inc., under NASA contract NAS 526555.

This project used public archival data from the Dark Energy Survey (DES). Funding for the DES Projects has been provided by the U.S. Department of Energy, the U.S. National Science

Foundation, the Ministry of Science and Education of Spain, the Science and Technology Facilities Council of the United Kingdom, the Higher Education Funding Council for England, the National Center for Supercomputing Applications at the University of Illinois at Urbana-Champaign, the Kavli Institute of Cosmological Physics at the University of Chicago, the Center for Cosmology and Astro-Particle Physics at the Ohio State University, the Mitchell Institute for Fundamental Physics and Astronomy at Texas A&M University, Financiadora de Estudos e Projetos, Fundação Carlos Chagas Filho de Amparo à Pesquisa do Estado do Rio de Janeiro, Conselho Nacional de Desenvolvimento Científico e Tecnológico and the Ministério da Ciência, Tecnologia e Inovação, the Deutsche Forschungsgemeinschaft, and the Collaborating Institutions in the Dark Energy Survey. The Collaborating Institutions are Argonne National Laboratory, the University of California at Santa Cruz, the University of Cambridge, Centro de Investigaciones Energéticas, Medioambientales y Tecnológicas-Madrid, the University of Chicago, University College London, the DES-Brazil Consortium, the University of Edinburgh, the Eidgenössische Technische Hochschule (ETH) Zürich, Fermi National Accelerator Laboratory, the University of Illinois at Urbana-Champaign, the Institut de Ciències de l'Espai (IEEC/CSIC), the Institut de Física d'Altes Energies, Lawrence Berkeley National Laboratory, the Ludwig-Maximilians Universität München and the associated Excellence Cluster Universe, the University of Michigan, the National Optical Astronomy Observatory, the University of Nottingham, The Ohio State University, the OzDES Membership Consortium, the University of Pennsylvania, the University of Portsmouth, SLAC National Accelerator Laboratory, Stanford University, the University of Sussex, and Texas A&M University. Based in part on observations at Cerro Tololo Inter-American Observatory, National Optical Astronomy Observatory, which is operated by the Association of Universities for Research in Astronomy (AURA) under a cooperative agreement with the National Science Foundation.

Facilities: Magellan:Baade (IMACS), GALEX, Parkes, Blanco

Software: astropy (Astropy Collaboration et al. 2013, 2018), ASTROMETRY.NET (Lang et al. 2010) The IDL Astronomy User's Library (Landsman 1993), DAOPHOT (Stetson 1987, 1994), SCAMP (Bertin 2006), SWARP (Bertin 2010).

ORCID iDs

David J. Sand  <https://orcid.org/0000-0003-4102-380X>
 Burçin Mutlu-Pakdil  <https://orcid.org/0000-0001-9649-4815>
 Michael G. Jones  <https://orcid.org/0000-0002-5434-4904>
 Ananthan Karunakaran  <https://orcid.org/0000-0001-8855-3635>
 Feige Wang  <https://orcid.org/0000-0002-7633-431X>
 Jinyi Yang  <https://orcid.org/0000-0001-5287-4242>
 Anirudh Chiti  <https://orcid.org/0000-0002-7155-679X>
 Paul Bennet  <https://orcid.org/0000-0001-8354-7279>
 Denija Crnojević  <https://orcid.org/0000-0002-1763-4128>
 Kristine Spekkens  <https://orcid.org/0000-0002-0956-7949>

References

- Abbott, T. M. C., Adamów, M., Aguena, M., et al. 2021, *ApJS*, 255, 20
 Adams, E. A. K., Giovanelli, R., & Haynes, M. P. 2013, *ApJ*, 768, 77
 Applebaum, E., Brooks, A. M., Christensen, C. R., et al. 2021, *ApJ*, 906, 96
 Astropy Collaboration, Robitaille, T. P., Tollerud, E. J., et al. 2013, *A&A*, 558, A33
 Astropy Collaboration, Price-Whelan, A. M., Sipőcz, B. M., et al. 2018, *AJ*, 156, 123
 Babul, A., & Rees, M. J. 1992, *MNRAS*, 255, 346
 Bellazzini, M., Beccari, G., Battaglia, G., et al. 2015, *A&A*, 575, A126
 Benítez-Llambay, A., Navarro, J. F., Abadi, M. G., et al. 2013, *ApJL*, 763, L41
 Bennet, P., Sand, D. J., Crnojević, D., et al. 2019, *ApJ*, 885, 153
 Bennet, P., Sand, D. J., Crnojević, D., et al. 2020, *ApJL*, 893, L9
 Bennet, P., Sand, D. J., Crnojević, D., et al. 2017, *ApJ*, 850, 109
 Bennet, P., Sand, D. J., Crnojević, D., et al. 2022, *ApJ*, 924, 98
 Benson, A. J., Frenk, C. S., Lacey, C. G., Baugh, C. M., & Cole, S. 2002, *MNRAS*, 333, 177
 Bernard, E. J., Monelli, M., Gallart, C., et al. 2009, *ApJ*, 699, 1742
 Bertin, E. 2006, in ASP Conf. Ser. 351, *Astronomical Data Analysis Software and Systems XV*, ed. C. Gabriel et al. (San Francisco, CA: ASP), 112
 Bertin, E. 2010, *SWarp: Resampling and Co-adding FITS Images Together*, Astrophysics Source Code Library, ascl:1010.068
 Brooks, A. M., Kuhlen, M., Zolotov, A., & Hooper, D. 2013, *ApJ*, 765, 22
 Brown, T. M., Tumlinson, J., Geha, M., et al. 2014, *ApJ*, 796, 91
 Buck, T., Macciò, A. V., Dutton, A. A., Obreja, A., & Frings, J. 2019, *MNRAS*, 483, 1314
 Bullock, J. S., & Boylan-Kolchin, M. 2017, *ARA&A*, 55, 343
 Bullock, J. S., Kravtsov, A. V., & Weinberg, D. H. 2000, *ApJ*, 539, 517
 Carlin, J. L., Sand, D. J., Price, P., et al. 2016, *ApJL*, 828, L5
 Carlin, J. L., Sand, D. J., Muñoz, R. R., et al. 2017, *AJ*, 154, 267
 Carlin, J. L., Mutlu-Pakdil, B., Crnojević, D., et al. 2021, *ApJ*, 909, 211
 Carlsen, S. G., Greco, J. P., Beaton, R. L., & Greene, J. E. 2020, *ApJ*, 891, 144
 Carlsen, S. G., Greene, J. E., Peter, A. H. G., Beaton, R. L., & Greco, J. P. 2021, *ApJ*, 908, 109
 Cerny, W., Pace, A. B., Drlica-Wagner, A., et al. 2021, *ApJL*, 920, L44
 Cerny, W., Simon, J. D., Li, T. S., et al. 2022, arXiv:2203.11788
 Chiboucas, K., Jacobs, B. A., Tully, R. B., & Karachentsev, I. D. 2013, *AJ*, 146, 126
 Chiti, A., Frebel, A., Jerjen, H., Kim, D., & Norris, J. E. 2020, *ApJ*, 891, 8
 Chiti, A., Frebel, A., Simon, J. D., et al. 2021, *NatAs*, 5, 392
 Crnojević, D., Sand, D. J., Zaritsky, D., et al. 2016a, *ApJL*, 824, L14
 Crnojević, D., Sand, D. J., Caldwell, N., et al. 2014, *ApJL*, 795, L35
 Crnojević, D., Sand, D. J., Spekkens, K., et al. 2016b, *ApJ*, 823, 19
 Crnojević, D., Sand, D. J., Bennet, P., et al. 2019, *ApJ*, 872, 80
 Davis, A. B., Nierenberg, A. M., Peter, A. H. G., et al. 2021, *MNRAS*, 500, 3854
 de Jong, J. T. A., Harris, J., Coleman, M. G., et al. 2008, *ApJ*, 680, 1112
 Dekel, A., & Silk, J. 1986, *ApJ*, 303, 39
 Dey, A., Schlegel, D. J., Lang, D., et al. 2019, *AJ*, 157, 168
 Díaz-Giménez, E., & Zandivarez, A. 2015, *A&A*, 578, A61
 Diemer, B., & Kravtsov, A. V. 2015, *ApJ*, 799, 108
 Dotter, A., Chaboyer, B., Jevremović, D., et al. 2008, *ApJS*, 178, 89
 Dressler, A., Hare, T., Bigelow, B. C., & Osip, D. J. 2006, *Proc. SPIE*, 6269, 62690F
 El-Badry, K., Wetzel, A., Geha, M., et al. 2016, *ApJ*, 820, 131
 Engler, C., Pillepich, A., Pasquali, A., et al. 2021, *MNRAS*, 507, 4211
 Frings, J., Macciò, A., Buck, T., et al. 2017, *MNRAS*, 472, 3378
 Geha, M., Wechsler, R. H., Mao, Y.-Y., et al. 2017, *ApJ*, 847, 4
 Giovanelli, R., Haynes, M. P., Adams, E. A. K., et al. 2013, *AJ*, 146, 15
 Hargis, J. R., Albers, S., Crnojević, D., et al. 2020, *ApJ*, 888, 31
 Iglesias-Páramo, J., Buat, V., Takeuchi, T. T., et al. 2006, *ApJS*, 164, 38
 Jeon, M., Besla, G., & Bromm, V. 2017, *ApJ*, 848, 85
 Jordi, K., Grebel, E. K., & Ammon, K. 2006, *A&A*, 460, 339
 Kalberla, P. M. W., & Haud, U. 2015, *A&A*, 578, A78
 Kalberla, P. M. W., McClure-Griffiths, N. M., Pisano, D. J., et al. 2010, *A&A*, 521, A17
 Karachentsev, I. D., Karachentseva, V. E., Huchtmeier, W. K., & Makarov, D. I. 2004, *AJ*, 127, 2031
 Karachentsev, I. D., Sharina, M. E., Makarov, D. I., et al. 2002, *A&A*, 389, 812
 Karunakaran, A., Spekkens, K., Oman, K. A., et al. 2021, *ApJL*, 916, L19
 Klypin, A., Zhao, H., & Somerville, R. S. 2002, *ApJ*, 573, 597
 Landsman, W. B. 1993, in ASP Conf. Ser. 52, *Astronomical Data Analysis Software and Systems II*, ed. R. J. Hanisch, R. J. V. Brissenden, & J. Barnes (San Francisco, CA: ASP), 246
 Lang, D., Hogg, D. W., Mierle, K., Blanton, M., & Roweis, S. 2010, *AJ*, 139, 1782
 Lavery, R. J., & Mighell, K. J. 1992, *AJ*, 103, 81
 Lee, J. C., Gil de Paz, A., Kennicutt, R. C. J., et al. 2011, *ApJS*, 192, 6
 Mac Low, M.-M., & Ferrara, A. 1999, *ApJ*, 513, 142
 Madore, B. F., & Freedman, W. L. 1995, *AJ*, 109, 1645

- Makarov, D., Makarova, L., Sharina, M., et al. 2012, *MNRAS*, **425**, 709
- Mao, Y.-Y., Geha, M., Wechsler, R. H., et al. 2021, *ApJ*, **907**, 85
- Martin, D. C., Fanson, J., Schiminovich, D., et al. 2005, *ApJL*, **619**, L1
- Martin, N. F., de Jong, J. T. A., & Rix, H.-W. 2008, *ApJ*, **684**, 1075
- Mau, S., Cerny, W., Pace, A. B., et al. 2020, *ApJ*, **890**, 136
- McClure-Griffiths, N. M., Pisano, D. J., Calabretta, M. R., et al. 2009, *ApJS*, **181**, 398
- McConnachie, A. W. 2012, *AJ*, **144**, 4
- McConnachie, A. W., & Irwin, M. J. 2006, *MNRAS*, **365**, 1263
- McConnachie, A. W., Huxor, A., Martin, N. F., et al. 2008, *ApJ*, **688**, 1009
- McQuinn, K. B. W., Skillman, E. D., Dolphin, A., et al. 2015, *ApJ*, **812**, 158
- Muñoz, R. R., Côté, P., Santana, F. A., et al. 2018, *ApJ*, **860**, 66
- Mutlu-Pakdil, B., Sand, D. J., Carlin, J. L., et al. 2018, *ApJ*, **863**, 25
- Mutlu-Pakdil, B., Sand, D. J., Crnojević, D., et al. 2021, *ApJ*, **918**, 88
- Mutlu-Pakdil, B., Sand, D. J., Crnojević, D., et al. 2022, *ApJ*, **926**, 77
- Putman, M. E., Zheng, Y., Price-Whelan, A. M., et al. 2021, *ApJ*, **913**, 53
- Rey, M. P., Pontzen, A., Agertz, O., et al. 2020, *MNRAS*, **497**, 1508
- Rhode, K. L., Salzer, J. J., Haurberg, N. C., et al. 2013, *AJ*, **145**, 149
- Ricotti, M., & Gnedin, N. Y. 2005, *ApJ*, **629**, 259
- Rodriguez Wimberly, M. K., Cooper, M. C., Fillingham, S. P., et al. 2019, *MNRAS*, **483**, 4031
- Sacchi, E., Richstein, H., Kallivayalil, N., et al. 2021, *ApJL*, **920**, L19
- Samuel, J., Wetzell, A., Chapman, S., et al. 2021, *MNRAS*, **504**, 1379
- Sand, D. J., Olszewski, E. W., Willman, B., et al. 2009, *ApJ*, **704**, 898
- Sand, D. J., Spekkens, K., Crnojević, D., et al. 2015a, *ApJL*, **812**, L13
- Sand, D. J., Strader, J., Willman, B., et al. 2012, *ApJ*, **756**, 79
- Sand, D. J., Crnojević, D., Strader, J., et al. 2014, *ApJL*, **793**, L7
- Sand, D. J., Crnojević, D., Bennet, P., et al. 2015b, *ApJ*, **806**, 95
- Saviane, I., Held, E. V., & Piotto, G. 1996, *A&A*, **315**, 40
- Sawala, T., Frenk, C. S., Fattahi, A., et al. 2016, *MNRAS*, **457**, 1931
- Schlafly, E. F., & Finkbeiner, D. P. 2011, *ApJ*, **737**, 103
- Simon, J. D. 2019, *ARA&A*, **57**, 375
- Simon, J. D., Brown, T. M., Drlica-Wagner, A., et al. 2021, *ApJ*, **908**, 18
- Skillman, E. D., Côté, S., & Miller, B. W. 2003, *AJ*, **125**, 593
- Smercina, A., Bell, E. F., Price, P. A., et al. 2018, *ApJ*, **863**, 152
- Smercina, A., Bell, E. F., Samuel, J., & D'Souza, R. 2022, *ApJ*, **930**, 69
- Stetson, P. B. 1987, *PASP*, **99**, 191
- Stetson, P. B. 1994, *PASP*, **106**, 250
- Tarumi, Y., Yoshida, N., & Frebel, A. 2021, *ApJL*, **914**, L10
- Teyssier, M., Johnston, K. V., & Kuhlen, M. 2012, *MNRAS*, **426**, 1808
- Tollerud, E. J., Geha, M. C., Grcevich, J., Putman, M. E., & Stern, D. 2015, *ApJL*, **798**, L21
- Tollerud, E. J., Geha, M. C., Grcevich, J., et al. 2016, *ApJ*, **827**, 89
- Tollerud, E. J., & Peek, J. E. G. 2018, *ApJ*, **857**, 45
- Toloba, E., Sand, D. J., Spekkens, K., et al. 2016, *ApJL*, **816**, L5
- Walsh, S. M., Willman, B., Sand, D., et al. 2008, *ApJ*, **688**, 245
- Weisz, D., & Boylan-Kolchin, M. 2019, *BAAS*, **51**, 1
- Weisz, D. R., Dolphin, A. E., Skillman, E. D., et al. 2014a, *ApJ*, **789**, 147
- Weisz, D. R., Dalcanton, J. J., Williams, B. F., et al. 2011, *ApJ*, **739**, 5
- Weisz, D. R., Zucker, D. B., Dolphin, A. E., et al. 2012, *ApJ*, **748**, 88
- Weisz, D. R., Skillman, E. D., Hidalgo, S. L., et al. 2014b, *ApJ*, **789**, 24
- Weisz, D. R., Dolphin, A. E., Martin, N. F., et al. 2019, *MNRAS*, **489**, 763
- Westmeier, T. 2018, *MNRAS*, **474**, 289
- Wetzell, A. R., Hopkins, P. F., Kim, J.-h., et al. 2016, *ApJL*, **827**, L23